# A New Method for Estimating Dermal Absorption from Chemical Exposure. 3. Compared with Steady-State Methods for Prediction and Data Analysis

**Annette L. Bunge,[1,3] Robert L. Cleek,[2] and Brent E. Vecchia[1]**

*Received July 20, 1994; accepted February 8, 1995*

***Purpose.*** This paper compares unsteady-state and steady-state methods for estimating dermal absorption or analyzing dermal absorption data. The unsteady-state method accounts for the larger absorption rates during short exposure times as well as the hydrophilic barrier which the viable epidermis presents to lipophilic chemicals. ***Methods.*** Example calculations for dermal absorption from aqueous solutions are presented for five environmentally relevant chemicals with molecular weights between 50 and 410 and $\log_{10}K_{ow}$ between 0.91 and 6.8: chloromethane, chloroform, chlordane, 2,3,7,8-TCDD, and dibenz(a,h)anthracene. Also, the new method is used to evaluate experimental procedures and data analyses of *in vivo* and *in vitro* permeation measurements. ***Results.*** In the five example cases, we show that the steady-state approach significantly underestimated the dermal absorption. Also, calculating permeability values from cumulative absorption data measured for exposure periods less than 18 times the stratum corneum lag time will overestimate the actual permeability. ***Conclusions.*** In general, steady-state predictions of dermal absorption will underestimate dermal absorption predictions which consider unsteady-state conditions. Permeability values calculated from data sets which include unsteady-state data will be incorrect. Strategies for analyzing *in vitro* diffusion cell experiments and confirming steady state are described.

**KEY WORDS:** dermal absorption; exposure assessment; percutaneous absorption; stratum corneum; permeability; octanol-water partitioning.

## INTRODUCTION

Estimates of systemic chemical exposure from dermal absorption should be based on the total mass absorbed including chemical that has entered but not yet left the stratum corneum (SC). Cleek and Bunge (1) describe a mathematical model for dermal absorption including unsteady-state effects and the hydrophilic barrier which the viable epidermis (EPI) presents to lipophilic compounds. Figure 1, taken from Cleek and Bunge (1), shows the normalized mass of chemical absorbed into the SC, $(M_{in}/(AL_cK_{cv}C_v^o))$ as a function of the dimensionless exposure time ($\tau = t_{exp}D_c/L_c^2$) for the SC-EPI composite membrane, assuming the vehicle concentration remains constant at $C_v^o$, the initial chemical concentration in the skin layers was zero, and the chemical concentration in the body system remains at zero during the entire exposure event. By plotting normalized $M_{in}$ against dimensionless $t_{exp}$, we can compare chemical exposures with different concentrations, exposure areas (A), or physicochemical properties (SC-vehicle partitioning $K_{cv}$, SC diffusivity $D_c$, and SC thickness $L_c$) on an equal basis. The parameter B measures the SC permeability relative to the EPI permeability and correlates with the lipophilic character as indicated by the octanol-water partition coefficient, $K_{ow}$.

As illustrated by the solid curves in Figure 1, the cumulative mass absorbed does not increase linearly in time, and the rate of mass absorption is not always constant, or steady. Specifically, during the early period of exposure, the absorption rate is proportional to $1/\sqrt{t_{exp}}$, meaning that at the onset of an exposure (i.e., at $t_{exp} = 0$) the absorption rate is infinitely rapid. The absorption rate decreases from this extremely large value to eventually reach the steady-state value. Once steady state is established, the normalized cumulative mass absorbed becomes linear in time. Even when steady state has been reached, the cumulative mass absorbed includes the mass absorbed during the unsteady-state period.

Permeability is an important quantity for characterizing the barrier properties of a membrane. Strictly, the permeability of a chemical through a membrane is only meaningful when measured at steady state. For skin including both the SC and EPI, the steady-state permeability of a chemical from a given vehicle v, $P_v$, depends on the steady-state permeabilities for the SC ($P_{cv}$) and EPI ($P_{ev}$):

$$\frac{1}{P_v} = \frac{1}{P_{cv}} + \frac{1}{P_{ev}} \tag{1}$$

which are defined as:

$$P_{cv} = \frac{K_{cv}D_c}{L_c} \tag{2}$$

$$P_{ev} = \frac{K_{ev}D_e}{L_e} \tag{3}$$

In Figure 1, $B = P_{cv}/P_{ev}$, and consequently $P_v$ is related to the SC only permeability according to:

$$P_v = \frac{P_{cv}}{1 + B} \tag{4}$$

Many *in vitro* and *in vivo* experiments on human and animal skins have been conducted to determine skin permeability of various chemicals. In some experiments, the amount of chemical absorbed was measured. In others, the amount of chemical or radioactivity which has crossed the skin barrier to appear in a receiving chamber, blood, or excreted materials (i.e., urine or feces) was determined. Since only the steady-state permeability has meaning, an important concern is whether *in vivo* or *in vitro* data were collected and analyzed to insure that a steady-state permeability value was obtained.

The mathematical expression plotted as the solid curves in Figure 1 is complex and impractical (1). However, Cleek

[1] Chemical Engineering and Petroleum Refining Department, Colorado School of Mines, Golden, Colorado 80401.

[2] Cox Laboratory for Biomedical Engineering, Rice University, Houston, Texas 77251.

[3] To whom correspondence should be addressed.

0724-8741/95/0700-0972$07.50/0 

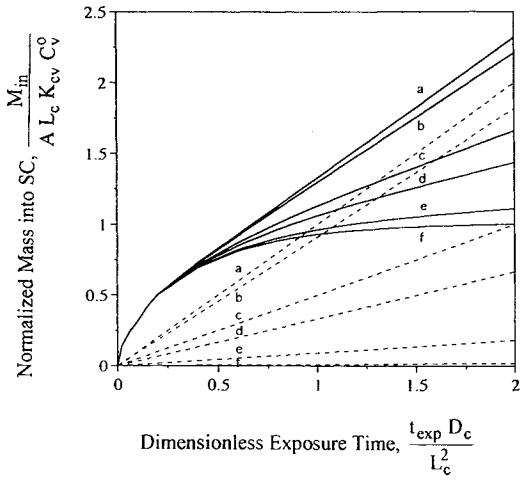


**Figure 1.** Normalized cumulative mass entering the stratum corneum when the viable epidermis is present plotted as a function of dimensionless $t_{exp}$ and B (a: $B \leq 0.01$; b: $B = 0.1$; c: $B = 1$; d: $B = 2$; e: $B = 10$; f: $B \geq 100$). Solid curves represent the unsteady-state case; dashed lines, the steady-state Eqn. (8).

and Bunge (1) have developed two simple algebraic expressions which closely approximate the curves in Figure 1. They also proposed an approach for estimating *a priori* the physicochemical parameters describing both the SC and EPI. The complete set of expressions, which we call the B-method, can be used to predict dermal absorption for a given exposure scenario. In addition, the B-method provides a simplified framework for comparing steady and unsteady-state analyses of experimental data and for evaluating the validity of resulting permeability values.

## THEORY

### The B-Method

The B-method approximately represents the solid curves in Figure 1 with algebraic expressions which are summarized in Table 1 (1,2). During the early absorption period (i.e., $t_{exp} < t^*$), the cumulative mass absorbed into the SC increases as a function of $\sqrt{t_{exp}}$, whereas after $t_{exp} > t^*$, the cumulative mass absorbed is linear in $t_{exp}$. The transition time $t^*$ represents the exposure time required to reach steady state. Notably, $t^*$ is related but not equivalent to the lag time ($t_{lag}$). Since the rate of absorption asymptotically approaches the steady-state rate, different values for $t^*$ are given depending on how closely one requires that the absorption rate approximate the steady-state rate. As a general rule, for chemicals with moderate to low lipophilicity, $t^*$ is approximately 2.4 $t_{lag}$.

Experimental values for either $D_c/L_c$ or $K_{cw}$ should not be mixed with estimates made from Eqns. (T9) or (T10) for the other parameter. These equations are internally consistent in that the product of the parameters in Eqns. (T9) and (T10) consistently estimates the steady-state SC permeability as predicted by Eqn. (T3).

The B-method estimate of the steady-state SC-EPI composite permeability, $P_v$, by Eqn. (4) includes contributions from both the SC and EPI and also indicates when one or the other completely controls absorption. As seen in Figure 1,

**Table 1. Summary of the B-Method Equations for Calculating the Cumulative Mass Absorbed**

For $t_{exp} \leq t^*$,

$$\frac{M_{in}}{A} = 2\,C_v^o K_{cv}\sqrt{\frac{D_c t_{exp}}{\pi}} \quad \text{(T1)}$$

For $t_{exp} > t^*$,

$$\frac{M_{in}}{A} = C_v^o\left[\frac{P_{cv}t_{exp}}{1+B} + K_{cv}L_c\frac{1+3B+3B^2}{3(1+B)^2}\right] \quad \text{(T2)}$$

$$\log_{10}P_{cw}\,(\text{cm/hr}) = -2.8-0.006(MW) + 0.74\log_{10}K_{ow} \quad \text{(T3)}$$

$$B = \frac{P_{cw}\sqrt{MW}}{(2.6\ \text{cm/hr})} \quad \text{(T4)}$$

For $B \leq 0.6$,

$$t^* = \frac{0.4\,L_c^2}{D_c} \quad \text{(T5)}$$

For $B > 0.6$,

$$t^* = (b - \sqrt{b^2 - c^2})\frac{L_c^2}{D_c} \quad \text{(T6)}$$

where b and c are defined as:

$$b = \frac{2}{\pi}(1+B)^2 - c \quad \text{(T7)}$$

$$c = \frac{1+3B+3B^2}{3(1+B)} \quad \text{(T8)}$$

$$\log_{10}(D_c/L_c,\ \text{cm/hr}) = -2.8-0.006(MW) \quad \text{(T9)}$$

$$\log_{10}K_{cw} = 0.74\log_{10}K_{ow} \quad \text{(T10)}$$

For aqueous vehicles, $K_{cv} = K_{cw}$.

For nonaqueous vehicles,

$$K_{cv} = K_{cw}K_{wv} \cong K_{cw}\frac{C_w^{sat}}{C_v^{sat}} \quad \text{(T11)}$$

the SC controls absorption when $B \leq 0.01$, the EPI controls when $B \geq 100$, and both the SC and EPI contribute to the barrier resistance when $0.01 < B < 100$. Likewise, when $B \leq 0.01$, Eqn. (4) predicts that $P_v = P_{cv}$ and when $B \geq 100$, Eqn. (4) predicts that $P_v = P_{ev}$. When B is between 0.01 and 100, Eqn. (4) predicts that the presence of the EPI alters the permeability of the SC-EPI composite even when the SC permeability is still smaller than the EPI permeability. That is, $P_v$ is less than $P_{cv}$ even when B (i.e., $P_{cw}/P_{ew}$) is as small as 0.01.

### Steady-State Method

Some researchers (references 3–5, to name only a few) have suggested calculating dermal absorption assuming steady state applies for all exposure times. That is,

$$\frac{M_{in}^{ss}}{A} = P_v C_v^o t_{exp} \quad (5)$$

In Eqn. (5), the permeability of the SC-EPI composite $P_v$ is either measured or estimated using a correlation such as Eqn. (T3) when the vehicle is water. Since Eqn. (T3) represents the steady-state permeability of the SC and not the SC-EPI composite, it will predict permeabilities for highly

lipophilic compounds which are higher than possible even if the SC is absent only the EPI remains. In this situation, Flynn (6) suggested comparing $P_{cw}$ calculated from a correlation such as Eqn. (T3) with an estimate of $P_{ew}$, usually taken to be between 0.1 and 1.0 cm/hr ($0.28 \times 10^{-4} - 2.8 \times 10^{-4}$ cm/s) (e.g., pp 4-21 and 5-12 in reference 7). Then, Flynn proposed:

$$P_w = P_{cw} \quad \text{when} \quad P_{cw} < P_{ew} \tag{6}$$

$$P_w = P_{ew} \quad \text{when} \quad P_{cw} \geq P_{ew} \tag{7}$$

Calculations made using the Flynn procedure, Eqns. (6) and (7), assume that only one of the skin layers, either the SC or the EPI, entirely controls permeation. In fact, for many lipophilic compounds, $P_{ew}$ is not much smaller than $P_{cw}$, meaning that both contribute significantly to the barrier resistance. In such situations, the skin barrier actually will be more resistant than indicated by assuming that $P_w$ equals only $P_{ew}$. In contrast, Eqn. (4) more accurately represents contributions from both the EPI and SC with exactly the same information as required by Eqns. (6) and (7): $P_{cw}$ and $P_{ew}$ (or $B = P_{cw}/P_{ew}$).

Consequently, we modify the steady-state expression, Eqn. (5), to include this improved representation for the combined SC-EPI permeability, Eqn. (4):

$$\frac{M_{in}^{ss}}{A} = \frac{P_{cv}C_v^o}{1 + B}\, t_{exp} \tag{8}$$

The normalized cumulative mass absorbed, $M_{in}^{ss}/(AL_cK_{cv}C_v^o)$, as calculated from Eqn. (8) is shown in Figure 1 as the dashed lines.

## APPLICATIONS AND DISCUSSION

Methods for estimating dermal absorption can be used in two distinctly different ways: (1) to predict absorption from either measured or estimated values of $K_{cv}$ and $D_c/L_c$, or (2) to analyze *in vivo* or *in vitro* experimental data to obtain values for $K_{cv}$ and $D_c/L_c$ separately or their product $K_{cv}D_c/L_c$ which equals $P_{cv}$. First, we will consider differences in predictions from the B and steady-state methods. In light of these results, we will then examine common experimental approaches and data analyses for determining permeability.

### Predicting Dermal Exposure

The comparison of unsteady and steady-state predictions in Figure 1 shows that the steady-state approach does not include the quicker absorption which occurs during the early exposure period while the SC reservoir is being filled. As a consequence, steady-state predictions of the cumulative mass absorbed are always less than would actually occur.

Figure 2 illustrates the predicted cumulative mass absorbed from aqueous solutions for dibenz(a,h)anthracene. Table 2 reports predictions for dibenz(a,h)anthracene and four other chemicals of environmental interest with widely varying MW and $K_{ow}$: chloromethane, chloroform, chlordane, and 2,3,7,8-TCDD. Table 2 also summarizes published and calculated parameters used in these predictions, including the approximate time to reach steady state (t*) and B.

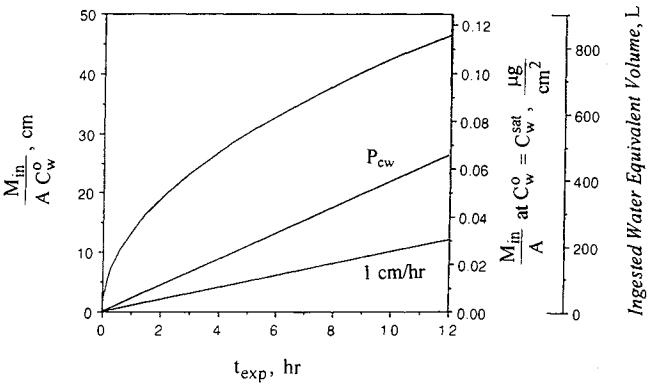


Figure 2. Cumulative mass of dibenz(a,h)anthracene absorbed into the SC as a function of $t_{exp}$ predicted by the B and steady-state expressions.

These calculations assumed that the chemical exposure was to aqueous solutions, that there was no depletion of chemical during the exposure, that skin permeation was rate controlling, and that the SC thickness was 0.001 cm.

The dermal absorption predictions in Figure 2 and Table 2 are reported in three different ways: (1) the mass absorbed normalized by the vehicle concentration, (2) the mass absorbed from a saturated aqueous solution, (3) and the volume of water of the same concentration that one must ingest to equal the estimated dermal exposure. The left hand axis in Figure 2 reports dermal absorption normalized by the aqueous concentration, $C_w^o$. The actual mass absorbed per area can be determined by multiplying plotted values by the known or estimated $C_w^o$.

The largest amount of absorption would occur at the largest possible concentration, that is at the saturation limit in water, $C_w^{sat}$. Furthermore, dermal absorption rates from any other saturated vehicle, the saturated vapor, or the neat chemical should all be the same as or less than from saturated water, provided that the vehicle or the chemical itself do not damage or alter the skin (15) and water is essentially insoluble in the neat chemical. (If the neat chemical has some water solubility, then absorption from a saturated aqueous solution will be less than from the neat chemical.) For lipophilic chemicals, the mass absorbed from water at $C_w^{sat}$, reported in Figure 2 as the leftmost of the two right hand axes, very nearly represents the maximum possible absorption of each chemical even from a neat solution. The assumptions that water is insoluble in the neat chemical, and that the neat chemical does not alter the skin will probably not be strictly valid for chloroform or chloromethane, which are not highly lipophilic and which may extract some of the lipid components from the SC. However, for these compounds, the exposure scenario of greatest concern is contact with aqueous solutions during showering, bathing or swimming and not with the neat chemical.

The rightmost of the right hand axes in Figure 2 reports the predicted dermal absorption in terms of the *Ingested Water Equivalent Volume* (IWEV). This is the volume of water one would have to drink to absorb a mass equivalent to immersing the entire body (18,000 $cm^2$) in an aqueous solution at the same concentration. Assuming 100% of the ingested chemical is absorbed and no chemical depletion in

Table 2. Example Estimates of Dermal Absorption from Aqueous Solutions

| | Chloromethane | Chloroform | Chlordane | 2,3,7,8-TCDD | dibenz(a,h)anthracene |
|---|---|---|---|---|---|
| $\log_{10}K_{ow}$ | 0.91 (7) | 1.90 (8) | 6.25 (9) | 6.80 (7) | 6.50 (10) |
| MW | 50.5 | 119.4 | 409.8 | 322 | 278.4 |
| $C_w^{sat}$ (25°C), mg/L | 4800 (11) | 7900 (12) | 0.056 (13) | $7.91 \times 10^{-6}$ (14) | $2.49 \times 10^{-3}$ (10) |
| B | 0.010 | 0.033 | 1.81 | 13.77 | 14.03 |
| $P_{cw}$, cm/hr | 0.0037 | 0.0078 | 0.232 | 2.00 | 2.19 |
| $P_{ew}$, cm/hr | 0.37 | 0.24 | 0.13 | 0.145 | 0.156 |
| $P_w$, cm/hr | 0.0037 | 0.0075 | 0.083 | 0.135 | 0.146 |
| $K_{cw}$ | 4.71 | 25.5 | $4.22 \times 10^4$ | $1.08 \times 10^5$ | $6.46 \times 10^4$ |
| $D_c$, $cm^2/hr$ | $7.89 \times 10^{-7}$ | $3.05 \times 10^{-7}$ | $5.51 \times 10^{-9}$ | $1.85 \times 10^{-8}$ | $3.39 \times 10^{-8}$ |
| $t_{lag}$, min | 12.7 | 32.8 | 1,815 | 540 | 295 |
| $t^*$, min | 30.4 | 78.8 | 7,330 (5.1 days) | 2,470 (1.7 days) | 1,350 (22.5 hrs) |
| $t_{exp}$, hr | 1 | 1 | 12 | 12 | 12 |
| $\frac{M_{in}}{AC_w^o}$, cm | *a 0.00527 | a 0.0159 | a 12.2 | a 57.4 | a 46.5 |
| | *b 0.0037 | b 0.0078 | b 2.78 | b 24 | b 26.3 |
| | *c na* | c na | c na | c 12 | c 12 |
| $\frac{M_{in}}{A}$ at $C_w^o = C_w^{sat}$, $\frac{\mu g}{cm^2}$ | a 25.3 | a 26 | a 0.686 | a 0.000454 | a 0.116 |
| | b 17.8 | b 61.6 | b 0.156 | b 0.00019 | b 0.0654 |
| | c na | c na | c na | c 0.000095 | c 0.0299 |
| #IWEV, L | a 0.0949 | a 0.286 | a 220 | a 1030 | a 837 |
| | b 0.0667 | b 0.140 | b 50.5 | b 432 | b 473 |
| | c na | c na | c na | c 216 | c 216 |

* a: B-Method; b: Steady-state, $P_{cw}$; c: Steady-state, $P_{cw}$ = 1.0 cm/h; na: not applicable.
# Ingested Water Equivalent Volume, Eq. (9).

the aqueous solution contacting the skin, a material balance shows that the ingested volume equivalent, $V_{ing}$, is related to dermal absorption according to:

$$V_{ing} = \left(\frac{M_{in}}{AC_w^o}\right)A \qquad (9)$$

where for Figure 2 and Table 2 ($M_{in}/AC_w^o$) is calculated from Eqns. (T1) and (T2) and A was taken as 18,000 $cm^2$. For smaller areas of exposure, $V_{ing}$ will be proportionally smaller. For example, an exposure of 10% of the body will correspond to 0.1 of the $V_{ing}$ from a whole body exposure. Presented in this way, the relative importance of the dermal and ingestion exposure routes are easily recognized. Specifically, when dermal and ingestion exposures are both possible, but $V_{ing}$ is larger than 2 L (the estimated daily volume for drinking water (16)), dermal absorption usually will represent the primary exposure risk.

In Figure 2 and Table 2, we compare calculations by the B and steady-state methods. For both methods $P_{cw}$ was estimated using Eq. (T3). The steady-state calculations, labeled as $P_{cw}$, were made using Eqn. (8) and assuming that B was always zero (i.e., $P_w = P_{cw}$). For two of the five chemicals (TCDD and dibenz(a,h)anthracene), the calculated $P_{cw}$ exceeded 1.0 cm/hr, which Flynn (6) estimated as the limiting permeability value of the SC-EPI composite. For these chemicals, we also report the steady-state prediction based on Flynn's recommendation, Eqn. (7), which is labeled as 1.0 cm/hr.

For chloromethane and chloroform, the most important exposure situations are bathing, showering or swimming in chlorine treated drinking water. Consequently, we report the mass absorbed over only one hour. In contrast, exposures to chemicals such as TCDD, chlordane, and dibenz(a,h)-anthracene are likely to be longer, so exposure periods up to 12 hours have been considered.

Chloromethane, the least lipophilic compound shown here ($\log_{10}K_{ow}$ = 0.91), is predicted to reach steady-state absorption after about 30 minutes. In contrast, the most lipophilic compound, TCDD ($\log_{10}K_{ow}$ = 6.8), does not reach steady state until almost 2 days of exposure. Chlordane, with its large MW, is not predicted to reach steady state for more than 5 days. The large difference in the time to reach steady state for chloromethane and chlordane arises because chlordane (MW = 409.8) diffuses much more slowly than does the smaller chloromethane (MW = 50.5). The deleterious effect which an increased MW has on permeability is evident from the relatively small increase (only about 60-fold) in $P_{cw}$ of chlordane over chloromethane despite a more than $10^5$ increase in $K_{ow}$.

We can draw some general conclusions, based on the results presented in Figure 2 and Table 2. First, the ingested water equivalent volumes are largest for the most lipophilic chemicals. For chemicals with large $K_{ow}$, water solubilities are so small that one would need to drink huge volumes to experience the same exposure level possible from dermal absorption. However, it is important to remember that the dermal absorption estimates assume constant vehicle concentration during the exposure: $C_w^o$ does not change. For chemicals with extremely low $C_w^{sat}$, this means that the skin must be able to contact large volumes of water. This might occur in a swimming, bathing or showering scenario. However, for smaller volume exposures such as occasional splashing, the volume of contact may be too small to main-

tain $C_w^o$ as a constant. Nevertheless, we can anticipate that the dermal exposure route may at least equal the ingestion route for highly lipophilic chemicals.

However, at the maximum exposure level, $C_w^o = C_w^{sat}$, the predicted cumulative mass absorbed for the larger $K_{ow}$ chemicals (e.g., chlordane, dibenz(a,h)-anthracene and TCDD), even after 24 hours, is much smaller than for the more moderate $K_{ow}$ compounds (chloromethane and chloroform) after an exposure of only 1 hour. Consequently, a large steady-state SC permeability from water does not imply a large dermal absorption rate. In fact, the maximum steady-state mass flux from water (and any other vehicle, vapor, or neat chemical, provided the skin is not altered and water is insoluble in the neat chemical) is $P_w C_w^{sat}$. In the case of chlordane, dibenz(a,h)anthracene, and especially TCDD, all of the increases in $P_w$ from a large $K_{ow}$ are more than offset by decreases in $C_w^{sat}$. For example, $C_w^{sat}$ for chloroform is 9 orders of magnitude larger than $C_w^{sat}$ for TCDD!

Finally, the steady-state approach for estimating dermal absorption always underpredicts the expected levels of absorption. The difference in the B and steady-state methods was greatest for the highest molecular weight compound. As we show later, the steady-state calculation will approach the B-method result for exposure times approaching about 18 $t_{lag,c}$ where $t_{lag,c}$ is the lag time across the SC. Since $t_{lag,c}$ increases with MW, at a specified $t_{exp}$ the largest MW chemical will be most poorly represented by the steady-state method. However, even for chloromethane (MW = 50), the steady-state prediction for a one hour exposure is about two-thirds of the amount expected when the early rapid absorption is included. For the highly lipophilic chemicals with $P_{cw}$ greater than 1.0 cm/hr (i.e., TCDD and dibenz(a,h)-anthracene), the steady-state calculation using the SC permeability ($P_{cw}$) rather than the SC-EPI composite permeability ($P_w \approx 1.0$ cm/hr) more closely predicts the actual mass absorbed. However, if the exposure continues long enough, the $P_{cw}$ steady-state prediction will eventually exceed the actual mass absorbed because the added resistance from the EPI has not been considered.

We have now compared the predictive application of the B and steady-state methods. An equally important application of these two methods is analysis of experimental data to calculate skin permeabilities, which we discuss next.

### Analyzing *in Vitro* Diffusion Cell Experiments

Skin permeability is frequently measured *in vitro* in a diffusion cell where skin is mounted between two solution chambers and solute transfer is followed by monitoring concentration in the receiving chamber. Typically, the cumulative mass of solute appearing in the receiving chamber is plotted as a function of time since the exposure began. Provided that the vehicle concentration remains essentially constant and that sink conditions are maintained in the receiving chamber, the cumulative mass of solute appearing in the receiving chamber eventually becomes linear in time, indicating that steady state has been established. The permeability can then be calculated from the slope of the steady-state line (i.e., the slope = $P_v C_v^o$).

The B-method describes the mass absorbed, and is, therefore, not appropriate for describing the appearance of mass in the receiving chamber. However it is still useful, since it gives a means to examine if steady state has been reached. For example, in situations when the SC controls absorption, we can quantitatively evaluate whether an *in vitro* experiment measuring the cumulative mass appearing in the receiving chamber has been conducted long enough to be at steady state. The procedure is illustrated in Figure 3 and summarized in Table 3. The simulated data points in Figure 3 were generated by numerically imposing errors on calculated mass absorption values using random numbers from a uniformly distributed population with a mean of zero and a standard deviation of 10% of the calculated mass absorbed. The solid curve represents the true cumulative mass which would appear in the receiving chamber as a function of time (1).

The permeability can be deduced from the slope of the line fitting the simulated cumulative mass absorption data normalized by $C_w^o$. Since the SC controls absorption in this example, the time-intercept of that line should represent the lag time for the SC, $t_{lag,c}$, which is theoretically equivalent to $L_c^2/(6D_c)$. Based on Eqn. (T5), any data points taken at times less than $t^* = 2.4\ t_{lag,c}$ should not be used to calculate the line representing the steady-state appearance of mass. An iterative process may be required as shown in Figure 3. The data are regressed to determine an apparent $t_{lag,c}$. This first regression may include data points which were at times less than $2.4\ t_{lag,c}$. These unsteady-state data points are then discarded and a new linear regression is made. This process is continued until no data taken at times less than $2.4\ t_{lag,c}$ are included in the linear regression. The slope of the resulting line is then equal to $P_{cw}$. For the case illustrated in Figure 3, the random variation in the simulated data causes $P_{cw}$ estimated by linear regression (0.00186 cm/hr) to be about 2% larger than the actual value (0.00183 cm/hr).

In situations where the SC does not control (i.e., when B is approximately 0.1 or larger and the EPI is present), then the graphically determined lag times include the contribution from the EPI as well as the SC. Vecchia (17) determined $t_{lag}$ for the SC-EPI composite barrier as:

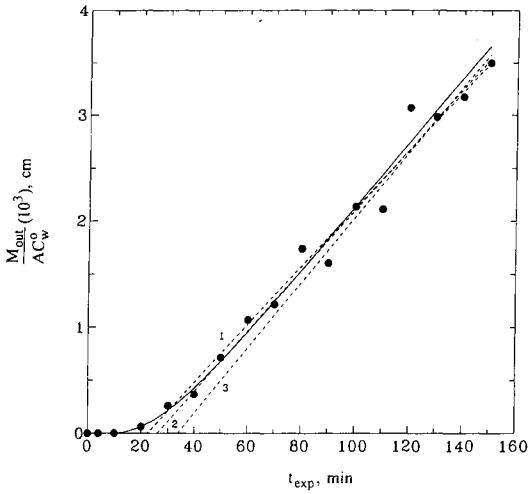


Figure 3. Illustrating the procedure for determining the steady-state SC permeability, $P_{cv}$, from an *in vitro* diffusion cell experiment measuring the cumulative mass appearing in the receiving chamber ($K_{ow}$ = 10, MW = 112.9, $P_{cw}$ = 0.00183 cm/h).

Table 3. Data from Steady-State Permeability Analysis in Figure 3

| Regression line no. | Data used | $t_{lag}$ (min) | $t^* = 2.4\ t_{lag}$ (min) | $P_w$ (cm/hr) |
|---|---|---|---|---|
| 1 | >20 min | 21.4 | 51.4 | 0.00159 |
| 2 | >70 min | 24.4 | 58.6 | 0.00166 |
| 3 | >90 min | 35.9 | 86.1 | 0.00186 |

$K_{ow}$ = 10
MW = 112.9
$L_c$ = 0.001 cm
$D_c$ = $3.33 \times 10^{-7}$ cm/hr
$t_{lag}$ = 30.0 min
$t^*$ = 72.0 min
B = 0.00748
$P_{cw}$ = 0.00183 cm/hr
$P_w$ = 0.00182 cm/hr
1 standard deviation corresponds to 10% error of the true value

$$t_{lag} = \left[\frac{1 + 3B}{6(1 + B)}\right]\frac{L_c^2}{D_c} = \frac{1 + 3B}{1 + B}\,t_{lag,c} \qquad (10)$$

when the lag time through the EPI ($t_{lag,e}$) is at least 10 times larger than $t_{lag,c}$ (which will always be the case unless the SC is damaged or the SC diffusivity is significantly enhanced otherwise). For lipophilic chemicals where B is larger than 0.6, Eqn. (10) and (T6) combine to give the time to approximately reach steady state:

$$t^* = (b - \sqrt{b^2 - c^2})\,\frac{6(1 + B)}{1 + 3B}\,t_{lag} \qquad (11)$$

where $t_{lag}$ is the lag time across the SC-EPI composite barrier, and b and c are defined by Eqns. (T7) and (T8) in Table 1.

Because lag times (either $t_{lag,c}$ or $t_{lag}$) increase with increasing MW, the time to reach steady state also increases with increasing MW. According to calculations made by Potts and Guy (18), it will take nonanol 28 times longer than methanol to reach steady state. Potts and Guy (18) also examined the effect of MW on apparent permeability measurements.

### Analyzing *in Vivo* Absorption Experiments

To derive permeability values from *in vivo* experiments which follow blood, urine or feces concentrations as a function of $t_{exp}$, one must include systemic pharmacokinetics in the analysis (e.g., reference 19). This requirement introduces additional experimentation and also uncertainties in the resulting percutaneous absorption parameters. Consequently, *in vivo* experiments which measure absorption directly have many advantages.

As already mentioned, for steady-state permeability values, experimental conditions must be at steady state, and therefore changes in the vehicle concentration must be small. (Steady-state $P_v$ can be deduced from experiments with varying vehicle concentration, provided that rate of concentration change is known and is small relative to the rate of dermal absorption.) The common *in vivo* experiment which deposits chemical dissolved in a volatile vehicle on the skin surface is therefore inappropriate for determining $P_v$, since $C_v$ changes rapidly and dramatically while the vehicle evaporates. Furthermore, the form of the deposited chemical after the vehicle evaporates (e.g., crystalline or amorphous solid or liquid), can profoundly but unaccountably affect absorption.

Only a few *in vivo* experiments have directly measured absorption while keeping $C_v$ essentially constant. A set of such experiments was recently reported for absorption of $^{14}$C-labeled tetrachloroethylene into hairless guinea pigs (20,21). The animals were immersed up to the neck in beakers of aqueous solution for 70 min and the amount of chemical remaining in the exposure solution was determined by liquid scintillation. Five replicate experiments were conducted. In each experiment, the first measurement was made at an exposure time of 10 min, and all reported values were normalized with respect to this first measurement. The initial concentrations, if known, were not reported. The 10 min concentrations were calculated from the net disintegrations per minute. Chemical loss from the exposure solution, modified for evaporation (which, as measured in separate control experiments, proved to be minor), was attributed to dermal absorption. Excretion efficiencies, measured by monitoring appearance of radioactivity in urine and fecal samples for 2 to 4 weeks following exposure, proved to be similar for dermal and subcutaneous delivery, supporting this assumption within the accuracy of the data.

Figure 4 shows the averaged cumulative mass absorbed (adjusted for differences in vehicle volumes and exposure areas) and one standard deviation for each time point plotted relative to the first measurement at 10 min ($t_{exp}$ − 10 min = 0). The cumulative mass absorbed is plotted relative to the mass absorbed at 10 min, normalized by the mass remaining in the vehicle at 10 min (i.e., $[M_{in}(\text{at } t_{exp}) - M_{in}(\text{at } t_{exp} = 10 \text{ min})]/[VC_w^o - M_{in}(\text{at } t_{exp} = 10 \text{ min})]$). Accordingly, a linear regression of steady-state data from Figure 4 is of the form:

$$\frac{[M_{in}(\text{at } t_{exp}) - M_{in}(\text{at } t_{exp} = 10 \text{ min})]}{VC_w^o\left[1 - \dfrac{M_{in}(\text{at } t_{exp} = 10 \text{ min})}{VC_w^o}\right]} = S\,(t_{exp} - 10 \text{ min}) + I \qquad (12)$$

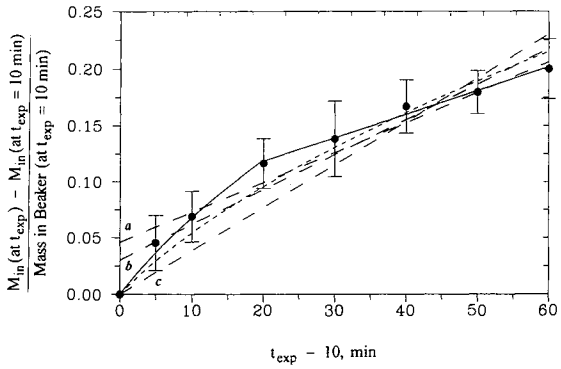


Figure 4. Cumulative mass of tetrachloroethylene dermally absorbed in hairless guinea pigs normalized with respect to the mass available for absorption 10 min after the exposure began.

After substituting the steady-state Eqn. (T2) for $M_{in}$ (at $t_{exp}$), the slope (S) and intercept (I) are defined as:

$$S = \frac{AP_{cw}}{V(1 + B)\left[1 - \frac{M_{in}\ (\text{at } t_{exp} = 10\ \text{min})}{VC_w^o}\right]} \quad (13)$$

$$I = \frac{AC_w^o\left[P_{cw}(10\ \text{min}) + L_c K_{cw}\left(\frac{1 + 3B + 3B^2}{3(1 + B)^2}\right)\right] - M_{in}\ (\text{at } t_{exp} = 10\ \text{min})}{VC_w^o\left[1 - \frac{M_{in}\ (\text{at } t_{exp} = 10\ \text{min})}{VC_w^o}\right]} \quad (14)$$

where A is the average area of exposure, and V is the average volume of solution in the beaker. Because Bogen *et al.* measured absorption relative to the absorption which occurred in the first 10 min, the mass absorbed in the first 10 min must be known or estimated to calculate the permeability from the slope. If steady state is achieved within the first 10 min of exposure, then $M_{in}$ (at $t_{exp}$ = 10 min) is represented by Eqn. (T2) and the intercept, I, should be approximately zero.

Figure 4 shows three different linear regressions (the dashed lines labeled as *a*, *b* and *c*), each implying different assumptions. The data point at $t_{exp}$ − 10 min = 0 was not included in the line *a* regression of the average cumulative mass absorbed values (S = 0.16 ± 0.06 $hr^{-1}$ and I = 0.046 + 0.043/−0.059), thereby making the assumption that all data, except the $t_{exp}$ − 10 min = 0 data point, are from exposure times longer than the time to reach steady state (i.e., 10 min < t* ≤ 15 min). The regressed S and I values are reported as the mean ± the 95% confidence interval. Unless noted otherwise, we report 95% confidence limits (lower 2.5% and upper 97.5%) determined by superimposing the normal distribution functions of S and I from regressions of each of the five animals (5000 trials for each animal were generated by Crystal Ball; see reference 22).

The line *c* regression (S = 0.23 $hr^{-1}$ ± 0.07) included all average cumulative mass absorbed data points while forcing I = 0. In this approach, the absorption rate is assumed to reach steady state prior to the first data point at $t_{exp}$ − 10 min = 0 (i.e., t* ≤ 10 min) with only a small error in the first measurement of the chemical mass remaining in the beaker (i.e., at $t_{exp}$ − 10 min = 0).

The line *b* regression included the first time point (i.e., $t_{exp}$ − 10 min = 0) while allowing I ≠ 0 (S = 0.19 ± 0.07 $hr^{-1}$ and I = 0.031 ± 0.042). When using this regression procedure, one has assumed that all data points (including the $t_{exp}$ − 10 min = 0 data point) were at steady state (i.e., t* ≤ 10 min), with a non-zero error in the measurement of the chemical mass remaining in the beaker at $t_{exp}$ − 10 min = 0. To the extent that measurement errors were randomly distributed, the magnitude of I should represent the error in the first measurement of chemical mass in the beaker. If all of the data points were at steady state, and the measurement error is random, we expect I for type *b* regression lines from replicate experiments to vary randomly around zero. The fact that I from all five replicates are positive supports our suspicion that steady state was not reached within the first 10 min.

For tetrachloroethylene, Bogen *et al.* (20,21) reported $P_{cw}$ = 0.37 (±0.13) cm/hr, calculated by averaging slopes from linear regressions of each of the five experiments (including all data points but not forcing I = 0) and assuming that $M_{in}$ (at $t_{exp}$ = 10 min) and B were both small (i.e., ≈ zero). Bogen *et al.* estimated this 95% confidence interval from the standard deviation of the permeability values for the five animals.

To calculate $P_{cw}$ from S, we must know $M_{in}$ (at $t_{exp}$ = 10 min). If, as Bogen *et al.* assumed, t* ≤ 10 min, then $M_{in}$ (at $t_{exp}$ = 10 min) is calculated from Eqn. (T2), leading to the conclusions that I = 0 in Eqn. (14), and that S in Eqn. (13) depends on the unknown value of ($K_{cw}L_c$) in addition to $P_{cw}$. Unfortunately, insufficient information is provided by Bogen *et al.* to estimate ($K_{cw}L_c$) separately from $P_{cw}$. If we arbitrarily assume that the chemical capacity of the SC is small (i.e., $K_{cw}L_c \approx 0$), then the mass absorbed relative to the initial mass in the beaker, $M_{in}$ (at $t_{exp}$ = 10 min)/($VC_w^o$) ≅ $AP_{cw}$ (10 min/60 min/hr)/V (the average V/A was 1.97 cm), and $P_{cw}$ = 0.36 cm/hr. Assuming that $M_{in}$ (at $t_{exp}$ = 10 min) ≈ 0, we calculated that $P_{cw}$ = 0.37 (±0.13) cm/hr, exactly as estimated by Bogen *et al.* (20,21). Since $\log_{10}K_{ow}$ = 3.40 for tetrachloroethylene, assuming B ≈ 0 is reasonable, but it is unlikely that the capacity of the SC is insignificant (i.e., $K_{cw}L_c \neq 0$). Consequently, $M_{in}$ (at $t_{exp}$ = 10 min)/($VC_w^o$) will be larger than estimated above, leading to smaller values for $P_{cw}$.

We assumed that t* > 10 min and used Eqn. (T1) to estimate $M_{in}$ (at $t_{exp}$ = 10 min)/($VC_w^o$) = 2 (A/V) $\sqrt{P_{cw} K_{cw}L_c/\pi}\ \sqrt{10\ \text{min}/60\ \text{min/hr}}$. Substituting this relationship into Eqns. (13) and (14), $P_{cw}$ and ($K_{cw}L_c$) can be deduced from S and I determined by linear regression of steady-state absorption values.

According to Eqn. (T1), any data points in Figure 4 at exposure times less than t* should be a function of $\sqrt{t_{exp}}$ rather than $t_{exp}$. Indeed, the early exposure data are much better predicted by the best fit $\sqrt{t_{exp}}$-curve (short dashed curve) in Figure 4 which was forced to be zero at time zero, providing evidence that Eqn. (T1) correctly represents unsteady-state absorption.

The data at the longer exposure times appear to be nearly linear with $t_{exp}$ suggesting that steady state was eventually established. Accordingly, we assumed various values for t*, and fit the data at which $t_{exp} \leq$ t* to a $\sqrt{t_{exp}}$-function, and the data at which $t_{exp}$ > t* to a linear function of $t_{exp}$. We iterated on t* until the residuals between the functions and data were minimized. The result, shown as the solid curve and line in Figure 4, suggests that the time to reach steady state is between the data points at 20 and 30 min (i.e., 10 min < t* − 10 min ≤ 20 min). If correct, this represents a $t_{lag}$ of between 8.3 and 12.5 min.

From the linear regressions for each animal when $t_{exp}$ − 10 min ≥ 20 min (S = 0.12 ± 0.10 $hr^{-1}$ and I = 0.077 + 0.070/−0.085), we determined $P_{cw}$ = 0.22 (±0.15) cm/hr and ($K_{cw}L_c$) = 0.90 (+0.44/−0.57) cm using Eqns. (13) and (14). We stochastically generated the mean and distribution functions for $P_{cw}$ and ($K_{cw}L_c$) separately for each animal using Crystal Ball (22) and assuming normal distribution functions for S and I (5000 trials for each animal). We then superimposed the distribution functions for $P_{cw}$ and ($K_{cw}L_c$) to de-

termine the mean values and the 95% confidence limits (i.e., lower 2.5% and upper 97.5%).

Using $P_{cw}$ = 0.22 cm/hr and $(K_{cw}L_c)$ = 0.90 cm, we estimate that $M_{in}$ (at $t_{exp}$ = 10 min)/$(VC_w^o) \approx 0.10$, which is more than ⅓ of the total amount absorbed in the entire 70 min exposure (i.e., $M_{in}$ (at $t_{exp}$ = 70 min)/$(VC_w^o) \approx 0.30$). The 0.37 (±0.13) cm/hr value calculated by Bogen *et al.* (20,21) is almost two times larger and significantly different than the $P_{cw}$ value of 0.22 (±0.15) cm/hr, calculated here using data from $t_{exp} \geq 30$ min and correcting for absorption during the first 10 min of exposure. As we prove shortly, calculating permeability coefficients from direct measurements of absorption which include unsteady-state data always overestimates the true permeability.

Using the same experimental procedures as for tetrachloroethylene, Bogen *et al.* (20,21) measured absorption of chloroform and trichloroethylene into guinea pigs. We have examined these data also and determined that, for these compounds (MW = 119.4 and 131.4 respectively for chloroform and trichloroethylene compared to 165.8 for tetrachloroethylene), t* for the guinea pig is approximately equal to or less than the time of their first data point at 10 min. Assuming t* for tetrachloroethylene is 20 to 30 min and adjusting for MW using Eqns. (T5) and (T9), we estimate that t* is between 10 and 16 min for chloroform and between 12 and 18 min for trichloroethylene which are reasonably consistent with our data analysis. Although Eqn. (T9) is for human rather than guinea pig SC, significant differences in the MW dependence are not expected.

A review of the literature indicates that time course data, like those in the guinea pig experiments just described, are quite unusual. More commonly, researchers report a single value of the cumulative mass absorbed in a given period of time. Since this cumulative mass measurement would include absorption during the unsteady-state period, the apparent permeability, $P_v^{app}$, calculated from:

$$P_v^{app} = \frac{M_{in}}{AC_v^o t_{exp}} \tag{15}$$

will always be larger than the true permeability $P_v$. This is illustrated in Figure 5 which plots the cumulative mass absorbed into the skin from an aqueous solution, normalized by the concentration $C_w^o$ and area of exposure A, as a function of time for a hypothetical chemical with properties listed in Table 3. The slopes of the dashed lines in Figure 5 correspond to $P_w^{app}$ values that would be obtained from the cumulative mass absorption measured for two experiments conducted at different $t_{exp}$ (20 and 80 min). The true permeability in this case is represented by the slope of the linear portion of the solid curve. The correct $P_w$ of 0.00182 cm/hr, is significantly less than $P_w^{app}$ of 0.0062 cm/hr based on the cumulative mass absorbed in 20 min, or 0.0032 cm/hr for 80 min.

This example may explain some of the reported differences between *in vitro* and *in vivo* experiments. Steady state is more easily confirmed in *in vitro* experiments, and therefore, permeability values from *in vitro* experiments are more likely to be steady-state values. Frequently, permeability coefficients calculated from *in vivo* experiments are larger than the true steady-state value because they are based on data

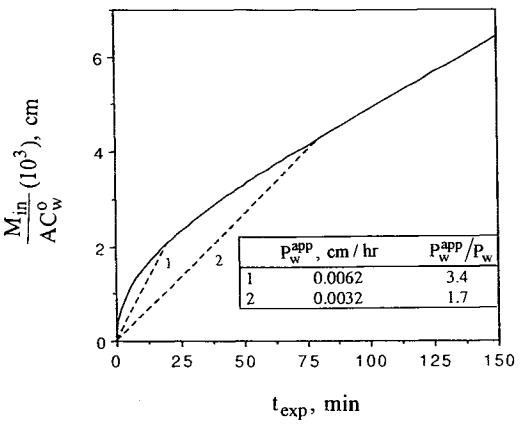


**Figure 5.** Illustrating the relationship between the actual steady-state permeability and the apparent permeability as estimated from the cumulative mass absorbed ($K_{ow}$ = 10, MW = 112.9, $P_{cw}$ = 0.00183 cm/h).

which include absorption during the unsteady-state period. A better approach for determining steady-state permeability coefficients from *in vivo* data is to use the rate of mass absorption once steady state has been achieved. That is,

$$P_v = \frac{1}{AC_v^o}\frac{dM_{in}}{dt_{exp}} \quad \text{for } t_{exp} > t^* \tag{16}$$

To use Eqn. (16) properly, steady state must be demonstrated which would require absorption data for no fewer than three exposure times. Even then, with data scatter, confirmation of steady state will be difficult.

If the exposure time is long enough (i.e., $t_{exp} > t^{\#}$), then the combination of the more rapid absorption during the unsteady-state period will be comparably small and the apparent permeability coefficient calculated from Eqn. (15) would be reasonably correct. How large does $t^{\#}$ need to be? This is easily estimated by calculating the exposure time $t^{\#}$ at which $M_{in}^{ss}/A$ from Eqn. (8) equals a specified fraction (F) of $M_{in}/A$ from Eqn. (T2):

$$t^{\#} = \frac{(1 + 3B)F}{3(1 - F)}\frac{L_c^2}{D_c} = \frac{2(1 + 3B)F}{(1 - F)}t_{lag,c} \tag{17}$$

Equation (17) is based on the SC lag time (i.e., $t_{lag,c} = L_c^2/(6D_c)$. When B is small, the steady-state estimate of the cumulative mass absorbed will predict less than 90% of the actual mass absorbed (i.e., $F < 0.9$) for exposure times less than 18 $t_{lag,c}$. For larger values of B, predictions of the cumulative mass absorbed from the steady-state equations will underestimate the actual absorption even for $t_{exp} > 18\ t_{lag,c}$. Estimates of the apparent permeability calculated according to Eqn. (15) will overestimate the actual steady-state $P_v$ by a factor of 1/F. Consequently, steady-state permeabilities calculated from cumulative mass absorption data will be within 10% of the actual permeability only if the experiment is conducted for $t_{exp} > 18\ t_{lag,c}$. The shorter the exposure time, the more $P_v^{app}$ will overestimate the actual $P_v$.

The relationship between $P_v^{app}$ calculated from Eqn. (15) and the actual steady-state $P_v$ can be estimated by substituting Eqns. (T1) and (T2) for $M_{in}/A$ into Eqn. (15) to yield:

$$\frac{P_v^{app}}{P_v} = (1 + B)\sqrt{\frac{24t_{lag,c}}{\pi t_{exp}}} \quad \text{for } t_{exp} \leq t^* \qquad (18)$$

$$\frac{P_v^{app}}{P_v} = 1 + \frac{2(1 + 3B)t_{lag,c}}{t_{exp}} \quad \text{for } t_{exp} > t^* \qquad (19)$$

where $t_{lag,c}$ is the lag time across only the SC. Strictly, these are only approximations, since Eqns. (T1) and (T2) are approximate representations of the curves in Figure 1 (albeit excellent representations especially for $t_{exp} \leq t^*$ and $B < 1$ (1)). Eqn. (19) is especially interesting since it shows that $P_v^{app}$ does not equal $P_v$ even though steady state has been reached (i.e., $t_{exp} > t^*$). This is because Eqn. (15) does not adjust for the more rapid rate of absorption during the shorter exposure times. Eqn. (15) incorrectly assumes that the absorption rate has been constant during the entire exposure.

Figure 6 shows $P_v^{app}/P_v$, Eqns. (18) and (19), as a function of $t_{exp}/t_{lag,c}$ for various values of B. Discontinuities arise at $t^*$ as the calculation switches from Eqn. (18) to (19), although these are barely visible. As expected, $P_v^{app}$ is always larger than $P_v$ and only approaches $P_v$ after long exposure times. For $t_{exp}$ of about $t_{lag,c}$, $P_v^{app}$ can be larger than $P_v$ by one or more orders of magnitude, depending on B. For highly lipophilic (large B) chemicals, the EPI chokes the chemical's penetration and the permeability across the SC-EPI composite barrier ($P_v$) is much smaller than $P_{cv}$. In addition, the SC capacity for chemical as reflected in $K_{cv}$ is large for highly lipophilic chemicals, so that the effect of the unsteady-state absorption period is more important when B is large. Finally, MW also affects $P_v^{app}/P_v$. Recall that $t_{lag,c}$ depends on $D_c$, and hence, the absorbing chemical's MW but not its $K_{ow}$. This means that the exposure time needed for $P_v^{app}$ to closely represent $P_v$ will be particularly long for a chemical with higher MW regardless of its lipophilic character (18).

To compare $P_v^{app}$ to the steady-state permeability of only the SC, as might be measured in an *in vitro* SC-only diffusion cell experiment or calculated from Eqn. (T3), we substitute Eqn. (4) into Eqns. (18) and (19) to obtain:

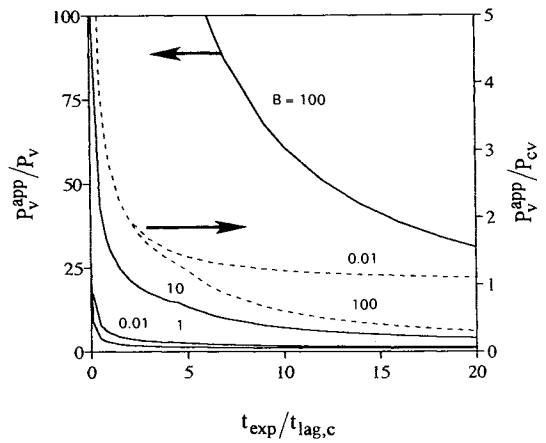


**Figure 6.** $P_v^{app}/P_V$ and $P_v^{app}/P_{cv}$ as functions of dimensionless $t_{exp}/t_{lag,c}$.

$$\frac{P_v^{app}}{P_{cv}} = \sqrt{\frac{24t_{lag,c}}{\pi t_{exp}}} \quad \text{for } t_{exp} \leq t^* \qquad (20)$$

$$\frac{P_v^{app}}{P_{cv}} = \frac{1}{1 + B}\left[1 + \frac{2(1 + 3B)t_{lag,c}}{t_{exp}}\right] \quad \text{for } t_{exp} > t^* \qquad (21)$$

The dashed curves referenced to the right hand axis of Figure 6 represent $P_v^{app}/P_{cv}$ as a function of $t_{exp}/t_{lag,c}$ for various values of B.

As for the $P_v^{app}/P_v$ curves, discontinuities appear from using the approximate representations of the unsteady-state absorption equations, (T1) and (T2). The discontinuities fall at different values for $t_{exp}/t_{lag,c}$ because $t^*$ is larger when B is 100 than when B is 0.01. For times less than $t^*$, $P_v^{app}/P_{cv}$ is independent of B because chemical absorption is completely controlled by the SC alone and any influence from the EPI is not felt. When $t_{exp}$ is larger than $t^*$, the B equal 0.01 and 100 curves separate. For highly lipophilic chemicals, the SC permeability, $P_{cv}$ will be larger than the true permeability for the SC-EPI composite, $P_v$. In this case $P_v^{app}$ eventually will be smaller than $P_{cv}$ and their ratio will become less than one. For more hydrophilic compounds, $P_v$ is approximately $P_{cv}$ and consequently, $P_v^{app}/P_{cv}$ will approach one at long exposure times. Most importantly, Figure 6 shows that when $t_{exp}$ is less than about 2 $t_{lag,c}$, $P_v^{app}/P_{cv}$ can be 2 or greater.

Results in Figures 5 and 6 may explain reported discrepancies between *in vitro* diffusion cell permeability coefficients and *in vivo* permeability coefficients calculated from the cumulative mass absorbed. In fact, the skin permeabilities in the *in vivo* and *in vitro* experiments could have been the same, but the apparent *in vivo* permeability was larger than its actual value because it was calculated from Eqn. (15) without a constant concentration exposure for at least 18 $t_{lag,c}$.

## CONCLUSIONS

A predictive approach, which we call the B-method, has been developed for estimating the cumulative mass absorbed during a dermal exposure including the faster rates during short exposures and the EPI resistance presented to lipophilic chemicals. Previous papers have developed the necessary equations and recommended procedures for estimating all of the required physicochemical data. In this paper, we have examined the B-method compared to steady-state methods for predicting absorption and for analyzing *in vitro* and *in vivo* data.

Example calculations are presented for dermal absorption from aqueous solutions for five chemicals with a wide range of MW (50.5 to 409.8) and $\log_{10}K_{ow}$ (0.91 to 6.80). These estimates are compared to predictions from the steady-state permeability approach, which underpredicts absorption in all the cases presented. If water is nearly insoluble in the neat chemical, then the maximum absorption rates occur at $C_w^{sat}$. For this group, the highly lipophilic chemicals at $C_w^{sat}$ absorb more slowly than less lipophilic chemicals because the increase in their permeabilities is more than offset by decreases in their $C_w^{sat}$. However, these low $C_w^{sat}$ decrease the risk from ingestion compared to dermal absorption.

Strictly, permeability coefficients are only meaningful when derived from steady-state data. Permeability coefficients calculated from data which include unsteady-state effects will not be correct. Based on the B-method, we have developed a procedure for confirming that *in vitro* permeability coefficients are calculated from data which are at steady state. A similar procedure is not possible for *in vivo* experiments. However, we do illustrate the effect of calculating apparent permeability coefficients from cumulative mass absorption data which include absorption during the unsteady-state period. The difference between the apparent and true permeability coefficient depends on the exposure time relative to the chemical's lag time. We show that $t_{exp}$ must be at least 18 $t_{lag,c}$ for the apparent permeability coefficient to be within 10% of the true permeability coefficient. Correct steady-state permeability coefficients may be determined from absorption rate data which are taken after steady state is achieved.

## NOMENCLATURE

- A = surface area of chemical exposure.
- b = parameter in t* calculation, Eqns. (T6) and (T7).
- B = parameter for the SC-EPI composite measuring the relative size of the SC permeability to the EPI permeability.
- c = parameter in t* calculation, Eqns. (T6), (T7) and (T8).
- $C_v^o$ = concentration of the absorbing chemical in the vehicle. Assumed to remain constant during the exposure period, $t_{exp}$.
- $C_v^{sat}$ = saturation concentration of the absorbing chemical in the vehicle.
- $C_w^o$ = concentration of the absorbing chemical in water. Assumed to remain constant during the exposure period, $t_{exp}$.
- $C_w^{sat}$ = saturation concentration of the absorbing chemical in water.
- $D_c$ = effective diffusivity of the absorbing chemical in the SC.
- $D_e$ = effective diffusivity of the absorbing chemical in the EPI.
- EPI = viable epidermis.
- F = fraction of the $M_{in}/A$ calculated from Eqn. (T2). Used in Eqn. (17).
- I = intercept of linear regressions of steady-state dermal absorption data. Defined in Eqns. (12) and (14).
- $K_{cv}$ = equilibrium partition coefficient between the SC and vehicle for the absorbing chemical.
- $K_{cw}$ = equilibrium partition coefficient between the SC and water for the absorbing chemical.
- $K_{ev}$ = equilibrium partition coefficient between the EPI and the vehicle for the absorbing chemical.
- $K_{ow}$ = octanol-water partition coefficient.
- $K_{wv}$ = equilibrium partition coefficient between water and the vehicle for the absorbing chemical.
- $L_c$ = effective thickness of the SC.
- $L_e$ = effective thickness of the EPI.
- $M_{in}$ = cumulative mass absorbed into the SC during an exposure period, $t_{exp}$.
- $M_{in}^{ss}$ = cumulative mass absorbed into the SC during an exposure period, $t_{exp}$, calculated from the steady-state Eqns. (5) and (8).
- MW = molecular weight of the absorbing chemical.
- $P_{cv}$ = steady-state permeability of the SC from a specified vehicle.
- $P_{cw}$ = steady-state permeability of the SC from water.
- $P_{ev}$ = steady-state permeability of the EPI from a specified vehicle.
- $P_v$ = steady-state permeability of the SC-EPI composite membrane from a specified vehicle.
- $P_v^{app}$ = apparent permeability estimated from the cumulative mass absorbed as given in Eqn. (15).
- $P_w$ = steady-state permeability of the SC-EPI composite membrane from water.
- S = slope of linear regressions of steady-state dermal absorption data. Defined in Eqns. (12) and (13).
- SC = stratum corneum.
- t* = time to approximately reach steady state. Estimations are given in Eqns. (T5) through (T8) and (11).
- $t^{\#}$ = time required for the steady-state calculation, Eqn. (8), to predict a specified fraction F of the amount which has actually absorbed as estimated by Eqn. (T2). Estimation is given in Eqn. (17).
- $t_{exp}$ = time period of exposure event.
- $t_{lag,c}$ = lag time across the SC, equals $D_c/(6L_c^2)$.
- $t_{lag}$ = lag time across the skin including both the SC and EPI, Eqn. (10).
- V = volume of solution in the exposure solution.
- $V_{ing}$ = ingested volume of water required to give an absorption equivalent to the dermal exposure.

## ACKNOWLEDGMENTS

This work was supported in part by the United States Environmental Protection Agency under Assistance Agreement Nos. CR817451 and CR822757. We thank R. Hertzberg, D.E. Burmaster, R.H. Guy, R.O. Potts, J. Parks, K. McCarley and K. Hoang for their helpful comments.

## REFERENCES

1. Cleek, R.L. and A.L. Bunge. A new method for estimating dermal absorption from chemical exposure. 1. General approach. *Pharm. Res.* **10**, 497-506 (1993).
2. Bunge, A.L. and R.L. Cleek. A new method for estimating dermal absorption from chemical exposure. 2. Effect of molecular weight and octanol-water partitioning. *Pharm. Res.* **12**, 87-94 (1995).
3. Yu, C.D., J.L. Fox, N.F.H. Ho, and W.I. Higuchi. Physical model evaluation of topical prodrug delivery—Simultaneous transport and bioconversion of vidarabine-5'-valerate I: Physical model development. *J. Pharm. Sci.* **68**, 1341-1346 (1979).
4. Turi, J.S., D. Danielson, and J.W. Woltersom. Effects of polyoxypropylene 15 stearyl ether and propylene glycol on percutaneous penetration rate of diflorasone diacetate. *J. Pharm. Sci.* **68**, 275-280 (1979).
5. Woodford, R. and B.W. Barry. Optimization and bioavailability of topical steroids: Thermodynamic control. *J. Invest. Derm.* **79**, 388-391 (1982).
6. Flynn, G. Physicochemical determinants of skin absorption. In *Principles of Route-to-Route Extrapolation for Risk Assess-*

*ment.* (T.R. Gerrity, C.J. Henry, Eds.) pp. 93-127, Elsevier, New York (1990).
7. US EPA. *Dermal Exposure Assessment: Principles and Applications.* Office of Health and Environmental Assessment, Washington, DC, EPA/600/8-91/011F (1992).
8. Banerjee, S., S.H. Yalkowsky, and S.C. Valvani. Water solubility and octanol/water partition coefficients of organics. Limitations of the solubility-partition coefficient correlation. *Environ. Sci. Tech.* **14**, 1227-1229 (1980).
9. Ellington, J.J. and F.E. Stancil. *Octanol/Water Partition Coefficients for Evaluation of Hazardous Waste Land Disposal: Selected Chemical.* U.S. Environmental Protection Agency, Athens, GA EPA/600/M-88/010 (1988).
10. Means, J.C., S.G. Wood, J.J. Hassett, and W.L. Banwart. Sorption of polynuclear aromatic hydrocarbons by sediment and soils. *Environ. Sci. Technol.* **14**, 1524-1528 (1980).
11. Karickhoff, S.W., L.A. Carreira, C. Melton, V.K. McDaniel, A.N. Vellino, D.E. Nute. *Computer prediction of chemical reactivity—the ultimate SAR,* US EPA, Athens, GA, EPA/600/M-89/017 (1989).
12. Seidel, A. *Solubilities of Organic Compounds,* D. van Nostrand, NY (1941).
13. Sanborn, J.R., R.L. Metcalf, W.N. Bruce, and P.Y. Lu. The fate of chlordane and toxaphene in a terrestrial-aquatic model ecosystem. *Environ. Entom.* **5**, 533-538 (1976).
14. Adams, W.J. and K.M. Blaine. A water solubility determination of 2,3,7,8-TCDD. *Chemosphere* **15**, 1397-1400 (1986).
15. Bunge, A.L., G.L. Flynn, and R.H. Guy. A predictive model for dermal exposure assessment. In *Drinking Water Contamination and Health: Integration of Exposure Assessment, Toxicology, and Risk Assessment* (R. Wang, Ed.) Marcell Dekker, New York, 347–374 (1994).
16. ICRP (Intl. Commission on Radiological Protection). *Report of the Task Group on Reference Man,* ICRP No. 23, Permagon Press, New York, NY (1975).
17. Vecchia, B. Personal communication, Colorado School of Mines, Golden, CO (1994).
18. Potts, R.O. and R.H. Guy. Drug transport across the skin and the attainment of steady-state flux. Proc. Intl. Symp. Control. Rel. Bioact. Mater. **21** (1994).
19. Silcox, G.D., G.E. Parry, A.L. Bunge, L.K. Pershing, and D.W. Pershing. Percutaneous absorption of benzoic acid across human skin II: Prediction of an *in vivo* skin flap system using *in vitro* parameters. *Pharm. Res.* **7**, 352–358 (1990).
20. Bogen, K.T., B.W. Colston, Jr., L.K. Machicao. Dermal absorption of dilute aqueous chloroform, trichloroethylene, and tetrachloroethylene in hairless guinea pigs. *Fund. Appl. Toxicol.* **18**, 30–39 (1992).
21. Bogen, K.T., B.W. Colston, Jr., L.K. Machicao. Percutaneous absorption of dilute aqueous chlorinated organic solvents in hairless guinea pigs. In *Drinking Water Contamination and Health: Integration of Exposure Assessment, Toxicology, and Risk Assessment* (R. Wang, Ed.) Marcell Dekker, New York, 323–346 (1994).
22. Crystal Ball, Version 3.0, Decisioneering, Inc., Denver, Colorado (1993).